INSTITUTE OF PHYSICS PUBLISHING JOURNAL OF PHYSICS B: ATOMIC, MOLECULAR AND OPTICAL PHYSICS

J. Phys. B: At. Mol. Opt. Phys. **38** (2005) S589–S604 doi:10.1088/0953-4075/38/9/010

Quantum control of light using electromagnetically induced transparency

A André[1], **M D Eisaman**[1], **R L Walsworth**[1,2], **A S Zibrov**[1,3] **and M D Lukin**[1]

[1] Physics Department, Harvard University, Cambridge, MA 02138, USA
[2] Harvard-Smithsonian Center for Astrophysics, Cambridge, MA 02138, USA
[3] Lebedev Institute of Physics, Moscow, 117924, Russia

Received 7 December 2004
Published 25 April 2005
Online at stacks.iop.org/JPhysB/38/S589

Abstract

We present an overview of recent theoretical and experimental work on the control of the propagation and quantum properties of light using *electromagnetically induced transparency* in atomic ensembles. Specifically, we discuss techniques for the generation and storage of few-photon quantum-mechanical states of light as well as novel approaches to manipulate weak pulses of light via enhanced nonlinear optical processes.

1. Introduction

Einstein's notions of reciprocity between stimulated absorption and emission and their relationship to spontaneous processes are central to the quantum theory of light–matter interactions. These ideas stimulated the development of the 'photon' concept and eventually paved the way for the field of quantum optics. Among the fundamental issues that are being addressed by modern quantum optical science is the extent to which such light–matter interactions can be controlled, both in principle and in practice.

In general, the strength of the interaction between light and atoms is a function of the frequency of light. When the light frequency matches the frequency of a particular atomic transition, a resonance condition occurs. In this case, the optical response of the medium is greatly enhanced. Light propagation is then accompanied by strong absorption and dispersion [1], as the atoms are actively promoted into fluorescing excited states. This is one of the consequences of the relation between stimulated and spontaneous emission rates. Research over the past few decades has shown, however, that this is not always the case. Specifically, under conditions of electromagnetically induced transparency (EIT), a resonant, opaque medium can be made transparent by means of interference [2].

To illustrate this effect, consider the situation shown in figure 1(a) in which the atoms have a pair of long-lived lower energy states $|g\rangle$ and $|s\rangle$. Such is the case for sublevels of different angular momentum (spin) states within the electronic ground state of alkali atoms.

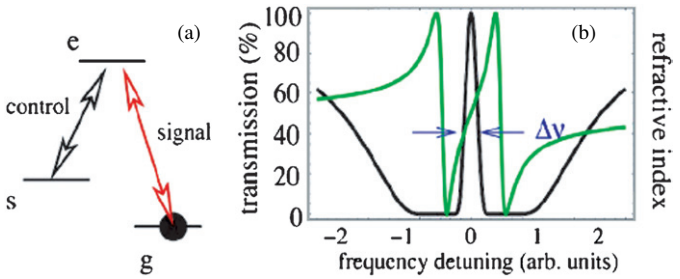

Figure 1. Electromagnetically induced transparency. (a) Prototype atomic system for EIT. (b) Spectrum of transmission and refractive index for signal field corresponding to EIT. Rapid variation of the refractive index (grey curve) causes a reduction of group velocity.

(This figure is in colour only in the electronic version)

In order to modify the propagation through this atomic medium of a light field that couples the ground state $|g\rangle$ to an electronically excited state $|e\rangle$ (the signal field), one can apply a second control field that is at resonance with the transition $|s\rangle \rightarrow |e\rangle$. The combined effect of these two fields is to stimulate the atoms into a so-called dark superposition of the states $|g\rangle$ and $|s\rangle$. In such a case, the two possible pathways in which light can be absorbed by atoms ($|g\rangle \rightarrow |e\rangle$ and $|s\rangle \rightarrow |e\rangle$) can interfere and cancel each other. The atoms are then said to be in dark states. With such destructive interference, none of the atoms are promoted to the excited state, leading to vanishing light absorption [2].

Many of the important properties of EIT result from the fragile nature of interference in a material that is initially opaque. Ideal transparency is attained only if the frequency difference between the two laser fields precisely matches the frequency separation between the atomic states. When the frequency difference is non-zero, the interference is not ideal and the medium becomes optically active. As a consequence, transparency is accompanied by steep dispersion of the refractive index, resulting in substantial reduction of the group velocity of light pulses in EIT medium [3–9]. Additionally, vanishing absorption is accompanied by an enhanced nonlinear response [10]. A variety of interesting manifestations and potential applications of EIT, ranging from single-cycle pulse generation [11] to nonlinear optics at ultra-low light level [12–15], have been demonstrated over the last decade. Thus, EIT has by now been firmly established as a powerful technique for coherent control of resonant propagation of classical light pulses.

At the same time, it is intriguing to consider if similar ideas can be extended to control pulses where quantum-mechanical properties of light become apparent. In particular, the ability to control quantum states as well as propagation properties of weak quantum signals, such as single-photon pulses, is central to the emerging field of quantum information science. It has been shown recently that EIT-based techniques can be used to create, store and manipulate single-photon pulses [8]. One of the particularly important potential applications of these techniques is in the area of long-distance quantum communication. This paper presents an overview of the recent work in this area.

2. Storing light pulses in EIT medium

2.1. Strong coupling of light and matter

Photons are robust and efficient carriers of quantum information, while atoms are well suited to precise quantum state manipulation. Quantum networks [16] require a technique for coherent

transfer of quantum states from photons to atoms and vice versa. Moreover, it is necessary to have a quantum memory that is capable of storing, releasing and manipulating quantum states at the level of individual quanta. Such coherent transfer techniques are essential, e.g., for quantum communication over long distances [17–20].

A conceptually simple approach to quantum memory is to store quantum states of single photons in individual atoms. This approach involves, in essence, coherent absorption and emission of single photons by single atoms. However, implementing this idea in practice is difficult: strong coupling of a single atom to a single cavity mode is required. Trapped atoms placed inside high-Q optical cavities offer an elegant approach to coherent light–atom interactions [21]. The spectacular experimental progress in this field, most notably by the groups of Kimble and Rempe [22–24], makes it a viable avenue for studying the fundamental physics of atom–photon interaction as well as for quantum networking with possibilities ranging from deterministic single-photon sources to quantum logic operations.

Recently, a number of protocols have been developed [25–28] that utilize a dispersive light–matter interaction and the ideas of quantum teleportation to achieve continuous-variable quantum state mapping into atomic samples. These ideas have been recently probed in pioneering experiments involving weak coherent state pulses [29].

In this paper, we focus on a set of techniques that uses coherent control of resonant atomic properties to store and manipulate photonic pulses via atomic memory.

2.2. Electromagnetically induced transparency (EIT)

EIT can be used to make a resonant, opaque medium transparent by means of quantum interference. In the case when the resonant control field is strong and its intensity is constant in time but the signal field is weak, the response of the atomic ensemble can be described in terms of the linear susceptibility spectrum $\chi(\omega)$,

$$\chi(\omega) = g^2 N \frac{\gamma_{gs} + \mathrm{i}\omega}{(\gamma_{ge} + \mathrm{i}\omega)(\gamma_{gs} + \mathrm{i}\omega) + |\Omega|^2} \tag{1}$$

where γ_{ij} corresponds to the relaxation rate of the $|i\rangle\langle j|$ coherence, Ω is the Rabi frequency of the control field (proportional to the electric field amplitude [1]), N is the total number of atoms in the sample, g is the atom–signal field coupling constant $g = \wp\sqrt{\frac{\omega_0}{2\hbar\epsilon_0 V}}$ ($\wp$ is the g–e dipole matrix element, ω_0 the g–e transition frequency, and V the quantization volume), and ω is the difference between the signal field frequency and the frequency of the atomic transition $|g\rangle \rightarrow |e\rangle$ (with $\omega \rightarrow 0$ corresponding to the exact atom–field resonance). The imaginary part of the susceptibility describes absorptive properties of the medium (thereby modifying the intensity transmission coefficient T), whereas the real part determines the refractive index n,

$$T(\omega) = \exp[-\mathrm{Im}\,\chi(\omega)kL], \qquad n(\omega) = 1 + \mathrm{Re}\,\chi(\omega)/2 \tag{2}$$

where L is the length of the medium. Ideal transparency is obtained in the limit when the relaxation of the low-frequency (spin) coherence vanishes ($\gamma_{gs} = 0$), in which case there is no absorption at atomic resonance (see figure 1(b)). Ideal transparency is attained only at exact resonance, i.e., when the frequency detuning $\omega = 0$. Away from this resonance condition, the interference is not ideal and the medium becomes absorbing. The transparency spike that appears in the absorption spectrum is typically very narrow (figure 1(b)), however the tolerance to frequency detuning (transparency window $\Delta\nu$) can be increased by using stronger coupling fields, since in this case interference becomes more robust.

Since atoms are decoupled from the light fields in an ideal EIT medium, at resonance the susceptibility vanishes, and the refractive index is equal to unity. This means that the

propagation velocity of a phase front (i.e., the phase velocity) is equal to that in vacuum. However, the narrow transparency resonance is accompanied by a very steep variation of the refractive index with frequency. As a result, the envelope of a wave packet propagating in the medium moves with a group velocity v_g [30], where

$$v_g = \frac{c}{1 + g^2 N/|\Omega|^2} \tag{3}$$

which can be much smaller than the speed of light in vacuum c [3, 7, 8]. Note that v_g depends on the control field intensity and the atomic density: decreasing the control power or increasing the atom density makes v_g slower, as demonstrated by Hau *et al* [4] and then by others [5, 6].

2.3. Dark-state polaritons

Consider the situation where the signal pulse is initially outside the medium. The front edge of the pulse then enters the medium and is rapidly decelerated. Being outside of the medium the back edge still propagates with vacuum speed c. As a result, upon entrance into the cell, the spatial extent of the pulse is compressed by the ratio c/v_g, while its peak amplitude remains unchanged. Clearly, the energy of the light pulse is much smaller when it is inside the medium. Photons are being expended to establish the coherence between the states $|g\rangle$ and $|s\rangle$, or, in other words, to change the atomic state, with the excess energy carried away by the control field. As the signal pulse exits the medium its spatial extent increases again and the atoms return to their original ground state; the pulse, however, is delayed as a whole by the group delay $\tau = \frac{L}{v_g} - \frac{L}{c}$.

Inside the medium, the wave of flipped spins propagates together with the signal pulse. The photons in the pulse are therefore strongly coupled to the atoms, with an associated quasiparticle called a dark-state polariton [30] that is a combined excitation of photons and spins. For the case when the decay rate of coherence between states $|g\rangle$ and $|s\rangle$ is negligible, we can describe the propagating signal by the electric field operator $\hat{\mathcal{E}}(z,t) = \sum_k \hat{a}_k(t)\,\mathrm{e}^{\mathrm{i}kz}$, where the sum is over the free-space photonic modes with wave vectors k and corresponding bosonic operators $\hat{a}_k$. To describe the properties of the medium, we use collective atomic operators $\hat{\sigma}_{\mu\nu}(z,t) = \frac{1}{N_z}\sum_{j=1}^{N_z} |\mu_j\rangle\langle\nu_j|\,\mathrm{e}^{-\mathrm{i}\omega_{\mu\nu}t}$ averaged over small but macroscopic volumes containing $N_z \gg 1$ particles at position z.

In particular, the operator $\hat{\mathcal{P}}(z,t) = \sqrt{N}\hat{\sigma}_{ge}(z,t)$ describes the atomic polarization oscillating at an optical frequency, whereas the operator $\hat{\mathcal{S}}(z,t) = \sqrt{N}\hat{\sigma}_{gs}(z,t)$ corresponds to a low-frequency spin wave. The control field is assumed to be strong and is treated classically. The atomic evolutionis governed by a set of Heisenberg equations: $\mathrm{i}\hbar\partial_t\hat{A} = [\hat{A}, \hat{H}]$, where $\hat{H}$ is the atom–field interaction Hamiltonian and $\hat{A} = \{\hat{\mathcal{P}}, \hat{\mathcal{S}}\}$. These equations can be simplified assuming that the signal field is weak and that Ω and $\hat{\mathcal{E}}$ change in time sufficiently slowly, i.e., adiabatically [31]. To leading order in the signal field $\hat{\mathcal{E}}$ we find

$$\hat{\mathcal{P}}(z,t) = -\frac{\mathrm{i}}{\Omega}\partial_t\hat{\mathcal{S}}, \qquad \hat{\mathcal{S}}(z,t) = -\frac{g\sqrt{N}\hat{\mathcal{E}}}{\Omega}. \tag{4}$$

The evolution of the signal field is described by the Heisenberg equation

$$\left(\frac{\partial}{\partial t} + c\frac{\partial}{\partial z}\right)\hat{\mathcal{E}}(z,t) = \mathrm{i}g\sqrt{N}\hat{\mathcal{P}}(z,t). \tag{5}$$

The solution of equations (4), (5) can be obtained by introducing a new quantum field $\hat{\Psi}(z,t)$ that is a superposition of photonic and spin-wave components:

$$\hat{\Psi}(z,t) = \cos\theta\hat{\mathcal{E}}(z,t) - \sin\theta\hat{\mathcal{S}}(z,t) \tag{6}$$

$$\cos\theta = \frac{\Omega}{\sqrt{\Omega^2 + g^2 N}}, \qquad \sin\theta = \frac{g\sqrt{N}}{\sqrt{\Omega^2 + g^2 N}}. \tag{7}$$

The field $\hat{\Psi}(z, t)$ obeys the equation of motion,

$$\left[\frac{\partial}{\partial t} + c\cos^2\theta \frac{\partial}{\partial z}\right]\hat{\Psi}(z, t) = 0, \tag{8}$$

which describes a shape-preserving propagation with velocity $v_g = c\cos^2\theta$ that is proportional to the magnitude of its photonic component.

2.4. Quantum memory using dynamic EIT

The idea for quantum memory is closely related to the dark-state polariton concept. When a polariton propagates in an EIT medium, it preserves its amplitude and shape,

$$\hat{\Psi}(z, t) = \hat{\Psi}\left[z - c\int_0^t \mathrm{d}\tau \cos^2\theta(\tau), t = 0\right] \tag{9}$$

but its properties can be modified by simply changing the intensity of the control beam. As the control intensity is decreased, $\cos^2\theta \sim |\Omega|^2$ becomes very small, and the group velocity is slowed. At the same time the contribution of photons to the polariton state is reduced. In particular, if the control beam is turned off ($\Omega(t) \to 0$), v_g is reduced to zero as $\theta(t) \to \pi/2$ and the polariton becomes purely atomic: $\hat{\Psi}(z, t) \to -\hat{\mathcal{S}}(z, t)$.

At this point, the photonic quantum state is mapped onto long-lived spin states of atoms (a 'spin wave'). As long as the storage process is sufficiently smooth [31], the entire procedure has no loss and is completely coherent. The stored photonic state can be easily retrieved by simply reaccelerating the stopped polariton by turning the control field back on. In recent years, it was shown experimentally that weak classical light pulses can be stored and retrieved in optically thick atomic media using dynamic EIT [32, 33], and that the storage process preserves phase coherence [34]. Also, a novel form of dynamic optical bistability was recently demonstrated experimentally [35]. Very recently, an experiment demonstrating quantum state transmission of an incident squeezed vacuum field through an EIT medium was carried out [36].

2.5. Stationary pulses of light

We now describe an extension of the above technique, which allows light propagating in a medium of warm Rb atoms to be converted into an excitation with localized, stationary electromagnetic energy, and then released after a controllable interval [37]. The key difference from the stored light technique described in the previous section is the application of both forward and backward control beams, after the input signal pulse has been mapped by dynamic EIT into an atomic spin wave (see figure 2). Upon their application, the counter-propagating control fields create a standing wave pattern, and EIT suppresses absorption of the signal pulse everywhere but in the nodes of the standing wave, resulting in a sharply peaked, periodic modulation of the atomic absorption for the signal light (figure 2(b)). Illumination by these beams also results in partial conversion of the stored atomic spin excitation into sinusoidally modulated signal light, but the latter cannot propagate in the medium due to Bragg reflections off the sharp absorption peaks, resulting in vanishing group velocity of the signal pulse, as in figure 2(d). Only after one of the control beams is turned off does the signal pulse acquire a finite velocity and leave the medium in the direction of the remaining control beam.

In the experimentally relevant case of small group velocities, there are two dark-state polariton components represented by $\hat{\Psi}_\pm = g\sqrt{N}\hat{\mathcal{E}}_\pm/\Omega_\pm$, where the control field consists of

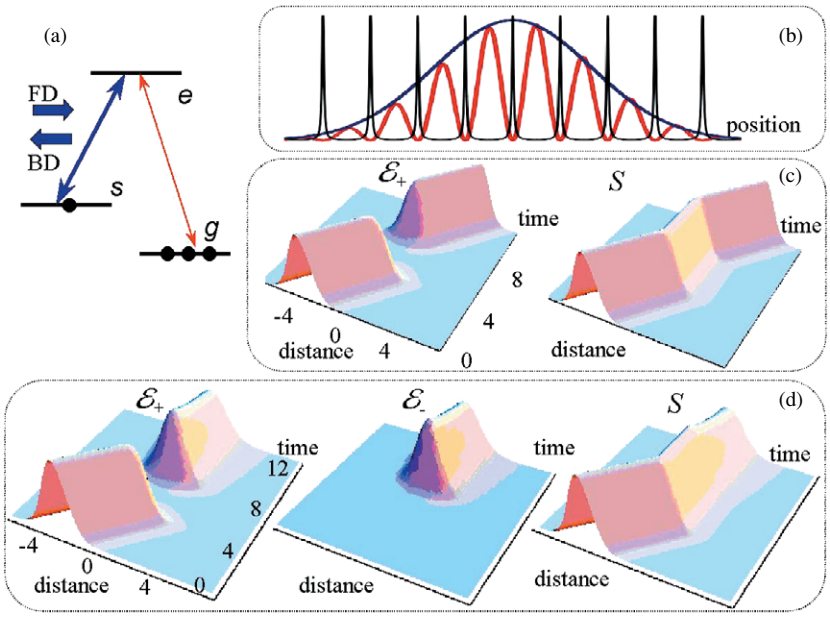

Figure 2. (a) Atomic level configuration. (b) Spatial variation of signal field absorption (black line), stationary pulse signal field (red line), and atomic spin coherence (blue line). (c) Storage of weak signal pulse in atomic coherence $|g\rangle\langle s|$. (d) Evolution of forward and backward signal components and atomic coherence when both control fields (FD and BD) are turned on with equal Rabi frequencies.

two counter-propagating fields with time-dependent Rabi frequencies $\Omega_{\pm}(t)$. In the adiabatic limit of slowly varying pulses, disregarding the slow decay of ground state coherence, and Fourier transforming ($\partial_t \to -\mathrm{i}\omega$), we find

$$c\frac{\partial}{\partial z}\hat{\Psi}_+ = \mathrm{i}\Delta K c\hat{\Psi}_+ + \mathrm{i}\eta\omega(\alpha_+\hat{\Psi}_+ + \alpha_-\hat{\Psi}_-) - \alpha_-\xi(\hat{\Psi}_+ - \hat{\Psi}_-) \tag{10a}$$

$$-c\frac{\partial}{\partial z}\hat{\Psi}_- = \mathrm{i}\Delta K c\hat{\Psi}_- + \mathrm{i}\eta\omega(\alpha_+\hat{\Psi}_+ + \alpha_-\hat{\Psi}_-) + \alpha_+\xi(\hat{\Psi}_+ - \hat{\Psi}_-) \tag{10b}$$

where $\eta = \frac{g^2N}{|\Omega_+|^2+|\Omega_-|^2}$, $\alpha_\pm = \frac{|\Omega_\pm|^2}{|\Omega_+|^2+|\Omega_-|^2}$, and $\xi = \frac{g^2N}{\gamma}$, and where ΔK is the wavevector mismatch between co-propagating signal and control fields. These equations describe two slow waves that are coupled due to periodic modulation of atomic absorption and group velocity. The terms containing ξ on the right-hand side of equations (10) are proportional to the absorption coefficient ξ near resonant line centre. When ξ is large these terms give rise to a pulse matching phenomenon [38]: whenever one of the fields is created the other will adjust itself within a short propagation distance to match its amplitude such that $\hat{\Psi}_+ - \hat{\Psi}_- \to 0$.

These ideas can be extended to three dimensions and lead to the localization of light pulses in all three spatial dimensions. In order to achieve three-dimensional (3D) confinement of light pulses, the transverse dependence of the control field intensity must be taken into account, resulting in a transverse variation of the index of refraction. For a focused control beam, the intensity decreases with distance from the optical axis, so that for negative two-photon detuning (as is necessary for phase-matching), the index of refraction decreases away from the optical axis. This leads to waveguiding of the signal light. Hence, in an optically dense medium ($\xi L/c \gg 1$) a stationary excitation confined in all three dimensions can be controllably created [40].

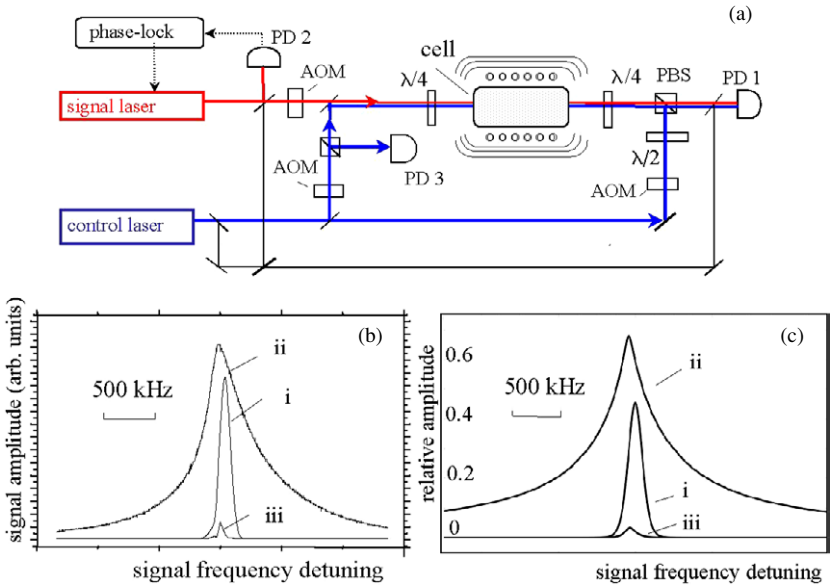

Figure 3. Experimental set-up (a) and results of CW experiments (b). (i) EIT signal transmission with FD on, (ii)–(iii) reflected and transmitted signal with both FD and BD on; (c) theoretical simulations of reflected and transmitted signals.

In a first set of experiments [37], we investigated the longitudinal confinement of light signals and the creation of stationary pulses of light. The experimental apparatus is shown in figure 3(a). We used a magnetically shielded 4 cm long ^{87}Rb vapour cell with density of 10^{12}–10^{13} cm^{-3}; long-lived hyperfine sublevels of the electronic ground state $S_{1/2}$ with $F = 1, 2$ served as the storage states $|g\rangle$, $|s\rangle$, respectively, coupled via the excited state $P_{1/2}$. The signal field is generated by an extended cavity diode laser and phase-locked to the control laser with a frequency offset corresponding to the hyperfine splitting of ^{87}Rb (6.84 GHz). PD1 and PD3 in figure 3(a) are fast photodiodes used for heterodyne detection of the signal, followed by a spectrum analyser.

We first consider continuous-wave (CW) excitation of the atomic Rb. Without the control beams the atomic medium is completely opaque to the forward signal beam. When the FD control field is present, a sharp, few 100 kHz wide resonance appears in the transmission spectrum of the signal beam, corresponding to EIT (curve (i) in figure 3(b)). Turning on the BD beam in the CW regime greatly reduces the EIT transmission (curve (iii)), while at the same time generating a reflected signal (up to ∼80%) beam that is detected in the backward direction (curve (ii)). These results demonstrate the possibility of coherent control (reflection and transmission) of light via simultaneous driving of the medium with FD and BD beams.

Turning to experiments with pulsed light, we first map the input signal pulse onto an atomic coherence of the Rb atoms, similarly to earlier stored light experiments [32, 33]. This procedure corresponds to figure 2(c) and its experimental observation is shown by curve (i) in figure 4(a). A Gaussian-shaped signal pulse of about 5 μs duration enters the medium where it is slowed to $v_g^0 \sim 6$ km s^{-1}. The FD control beam is then turned off; note that a fraction of the signal pulse leaves the cell before that, leading to the first peak of curve (i). When the FD control field is turned back on, the stored atomic excitation is converted back into light and detected in the forward direction (second peak of curve (i)). We next consider the retrieval of the atomic excitations by simultaneous application of the FD and BD control beams.

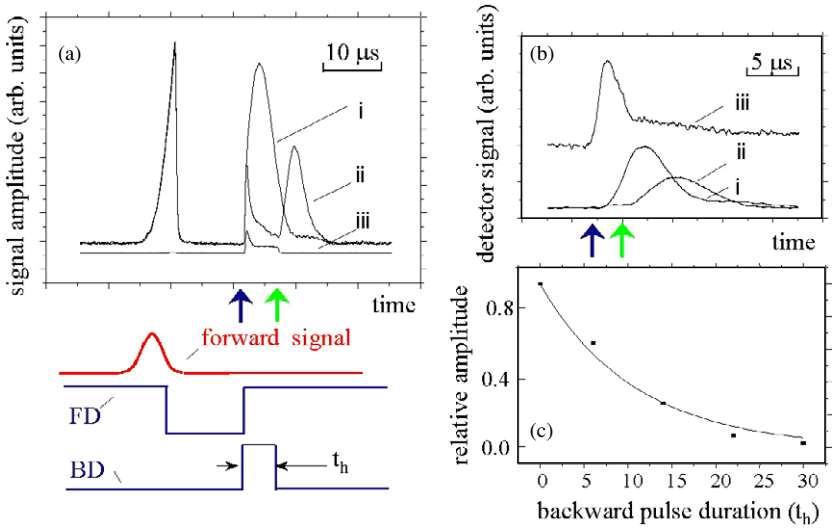

Figure 4. (a) Pulsed experiments, (i) storage and retrieval of signal in forward direction when FD is turned off then back on, (ii) same when FD and BD both turned on, (iii) signal in backward direction under the same conditions. (b) Rb fluorescence measured at the side of the cell, (iii) fluorescence associated with signal light during release with both FD and BD on. Curves (i) and (ii) (shown for reference) are the same as curves (i) and (ii) in figure 3(a). (c) Dependence of released signal magnitude on BD pulse duration t_h.

When the intensities of the beams are carefully adjusted, the output signal pulses in both forward and backward directions are greatly suppressed (curves (ii) and (iii) in figure 4(a)). Both channels exhibit small leakage. We attribute the first peak to photons retrieved near the cell boundaries, which do not experience sufficient Bragg reflections to be trapped efficiently. The long tail is likely due to a slow spreading of the stored pulse. When the BD beam is turned off the released pulse is detected in the forward channel (curve (ii)). The presence of signal light inside the cell during the simultaneous application of the two control beams was verified directly by monitoring fluorescence from the side of the cell (figure 4(b). Background fluorescence associated with control beams is subtracted. For times when the signal output in forward and backward directions is greatly suppressed, we observed significant enhancement of the signal light fluorescence (curve (iii) in figure 4(b)), due to residual atomic absorption.

These observations provide evidence for controlled conversion of the stored atomic coherence into a stationary photonic excitation in the cell. Note, in particular, that the magnitude of the fluorescence drops sharply after the BD pulse is turned off. This drop is followed by a gradual decay associated with the exit of the slow pulse from the medium. This behaviour is in qualitative agreement with our simple model, which predicts the light intensity in the stationary pulses to be double of that in the slowly propagating pulse.

3. Quantum state manipulation in atomic ensembles

3.1. Raman scattering for quantum state preparation

In this section, we describe a novel technique for generating pulses of light with controllable, well-defined photon numbers, propagation direction, timing and pulse shapes by exploiting

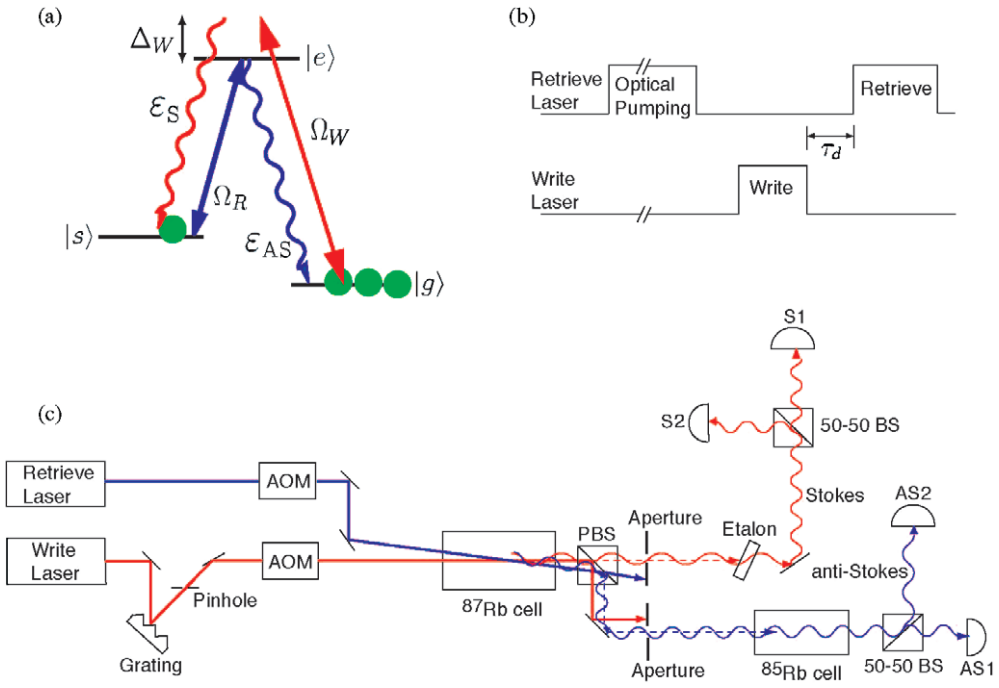

Figure 5. Experimental procedure and apparatus for quantum state generation via Raman scattering. (a) ^{87}Rb levels used in the experiments (D_1 line): $|g\rangle = |5^2S_{1/2}, F = 1\rangle, |s\rangle = |5^2S_{1/2}, F = 2\rangle$, and $|e\rangle$ corresponds to $|5^2P_{1/2}, F' = 1\rangle$ and $|5^2P_{1/2}, F' = 2\rangle$. (b) After the optical pumping pulse (provided by the retrieve laser), the 1.6 μs long write pulse is followed by the retrieve pulse after a controllable delay τ_d. (c) Schematic of the experimental set-up. For details see [43].

Raman preparation and retrieval of atomic excitations. This technique is particularly important in the contexts of long-distance quantum communication [18, 19] and EIT-based quantum nonlinear optics [10]. Following the early experiments by Kuzmich and co-workers [41] and van der Wal and co-workers [42], in which non-classical correlations were demonstrated, there has been exciting experimental progress in this area. Our approach, using Raman preparation and EIT-based retrieval of atomic excitations, has resulted in generation of single-photon pulses with controllable propagation direction, timing and pulse shapes [43, 44]. Concurrently, the experiments at Caltech [45, 46], have demonstrated non-classical photon pair creation and single-photon production via conditional measurement of the light from optically thick atomic ensembles. Also noteworthy are experiments demonstrating coherent quantum state transfer between matter and light using optically thick atomic ensembles [47], and experiments on low-light level four-wave mixing in atomic ensembles using EIT [48, 49].

The use of Raman scattering for non-classical light generation can be understood qualitatively by considering three atomic states coupled by a pair of optical control fields in a 'double-Λ' configuration (figure 5(a)). A large ensemble of atoms is initially prepared in the ground state $|g\rangle$. Atomic spin excitations are produced via spontaneous Raman scattering [50], induced by an off-resonant control beam with Rabi frequency Ω_W and detuning Δ, which we refer to as the write beam. In this process, correlated pairs of frequency-shifted photons (so-called Stokes photons) and flipped atomic spins are created (corresponding to atomic Raman transitions into the state $|s\rangle$). Energy and momentum conservation ensures that for each Stokes photon emitted in a particular direction, there exists exactly one flipped

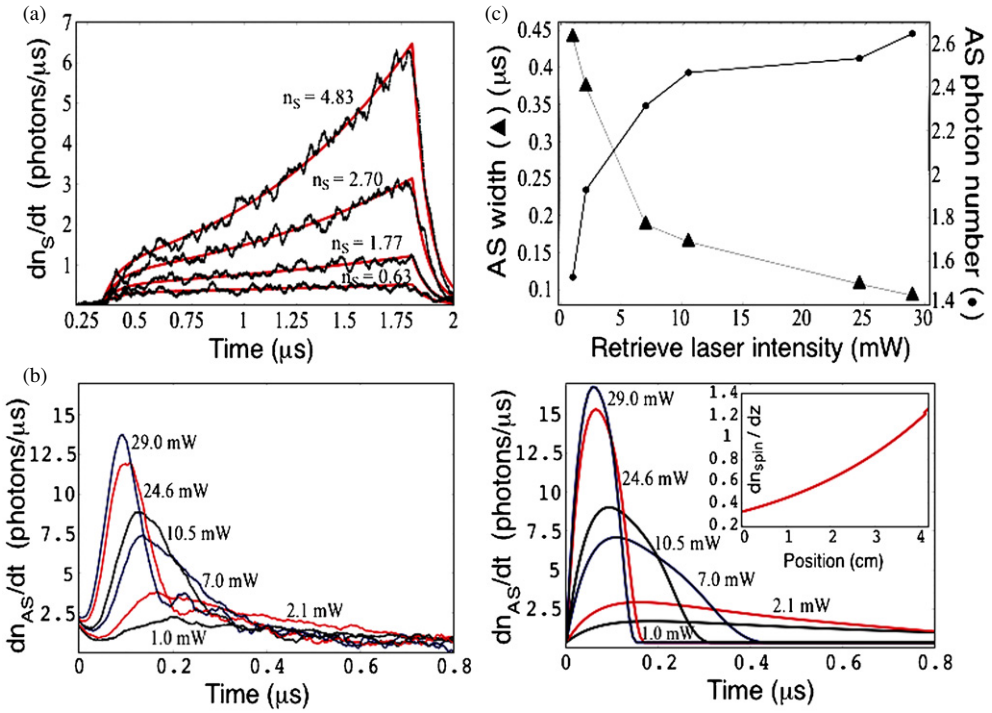

Figure 6. Stokes and anti-Stokes pulse shapes [43]. (a) Experimental and theoretical values of the Stokes photon flux dn_S/dt. (b) Experimental (left) and theoretical (right) values of the anti-Stokes photon flux dn_{AS}/dt. The experimental pulse shapes correspond to a Stokes pulse with $n_S \approx 3$ photons, and the theoretical curves assume an initial spin wave with $n_{\text{spin}} = 3$ excitations and an optical depth of $\simeq 20$. Each curve is labelled with the power of the retrieve laser. (b, inset) Theoretical calculation of the number of flipped spins per unit length dn_{spin}/dz (cm^{-1}) for $n_{\text{spin}} = 3$. (c) Measured anti-Stokes pulse width (full-width at half-max) and total photon number as a function of the retrieve laser intensity.

spin quantum in a well-defined spin-wave mode. As a result, the number of spin-wave quanta and the number of photons in the Stokes field are strongly correlated. These atom–photon correlations closely resemble those between two electromagnetic field modes in parametric down-conversion [51, 52].

Thus, measurement of the Stokes photon number n_S ideally projects the spin wave into a non-classical collective state with n_S spin quanta [19]. After a controllable delay time τ_d (see figure 5(b)), the stored spin wave can be coherently converted into a light pulse by applying a second near-resonant laser beam with Rabi frequency Ω_R (retrieve laser), see figure 5(a). The physical mechanism for this retrieval process is identical to that employed in our stored light experiments [33, 34]. The direction, delay time τ_d, and rate of retrieval are determined by the direction timing and intensity of the retrieve laser, allowing control over the spatio-temporal properties of the retrieved pulse (referred to as the anti-Stokes pulse).

3.2. Experiments on quantum control of few-photon pulses

We now describe in more detail our experiments on quantum correlated Stokes/anti-Stokes pulse production and single-photon generation. Figure 5(c) [42, 43] illustrates a typical experimental set-up recently used by our group. Figure 6(a) shows the average number of

detected Stokes photons per unit time (photon flux) in the write channel as a function of time during the 1.6 μs long write pulse. The photon flux is controlled by varying the excitation intensity. The shape of the Stokes pulse changes qualitatively as the total number of photons in the pulse exceeds unity: for pulses containing on average one photon or less, the flux is constant in time (more generally it follows the shape of the write laser), whereas for pulses containing more than one photon, the flux increases with time. This evolution of the Stokes pulses can be understood qualitatively by considering the mutual growth of the photon field and spin excitation: the first flipped spin *stimulates* subsequent spin excitations which are accompanied by increased probability of Stokes photon emission. The observed dynamics provide evidence for the collective nature of the atomic spin excitations.

After a time delay τ_d, we apply the retrieve beam to convert the stored spin wave into anti-Stokes photons. Figure 6(b) demonstrates that the duration and peak flux of the anti-Stokes pulse can be controlled via the intensity of the retrieve laser. The resonant retrieve laser converts the spin coherence into a dark-state polariton [30], and eventually into an anti-Stokes photon. Since the retrieve laser establishes an EIT configuration for the generated anti-Stokes field, for larger (smaller) retrieve laser intensity, the excitation is released faster (slower), while the amplitude changes in such a way that the total number of anti-Stokes photons is always equal to the number of spin-wave excitations. In practice, decay of the spin coherence reduces the total number of anti-Stokes photons that can be retrieved, as indicated by theoretical calculations (figure 6(b)) based on [30].

At fixed laser intensities and durations, the number of Stokes and anti-Stokes photons fluctuates from event to event in a highly correlated manner [42]. To quantify these correlations, we compare the number of Stokes and anti-Stokes photons for a large number of pulsed events (each with identical parameters). The variance of the resulting distributions is then compared to the theoretical photon shot noise level $\mathrm{PSN}_{\mathrm{th}} = \bar{n}_S + \bar{n}_{AS}$, which represents the maximum degree of correlations possible for classical states [54]. We experimentally determine photon shot noise $\mathrm{PSN}_{\mathrm{meas}} = \mathrm{var}(AS1 - AS2) + \mathrm{var}(S1 - S2)$ by using a 50–50 beam-splitter and two APDs per detection channel (see figure 5(c)).

To quantify the correlations, we consider the normalized variance $V = \mathrm{var}(\{n_{AS} - n_S\})/\mathrm{PSN}_{\mathrm{meas}}$, which is 1 for classically correlated pulses and zero for pulses exhibiting perfect number correlations. Figure 7(a) shows the normalized variance V as a function of storage time τ_d. Non-classical correlations ($V < 1$) between Stokes and anti-Stokes pulses are clearly observed for storage times up to a few microseconds. This time scale arises because non-classical correlations persist only as long as the coherence of the stored excitation is preserved. We note that at $\tau_d = 0$ the observed value $V = 0.942 \pm 0.006$ is far from the ideal value of $V = 0$. Sources of error contributing to this non-ideal value include finite retrieval efficiency, losses in the detection system, background photons, APD after-pulsing effects and imperfect mode matching.

3.3. Generation of non-classical states

Since the storage and retrieval processes ideally result in identical photon numbers in the Stokes and anti-Stokes pulses [53], this technique should allow preparation of an n-photon Fock state in the anti-Stokes pulse conditioned on detection of n Stokes photons. In practice, these correlations allow for the conditional preparation of an anti-Stokes pulse with intensity fluctuations that are suppressed compared with classical light. To quantify this preparation, we measured the second-order intensity correlation function $g^{(2)}_{n_S}(AS)$ and mean number of photons $\bar{n}^{AS}_{n_S}$ for the anti-Stokes pulse conditioned on the detection of n_S photons in the Stokes channel (see figure 7(b)). (For classical states of light, $g^{(2)} \geqslant 1$; an ideal Fock state with

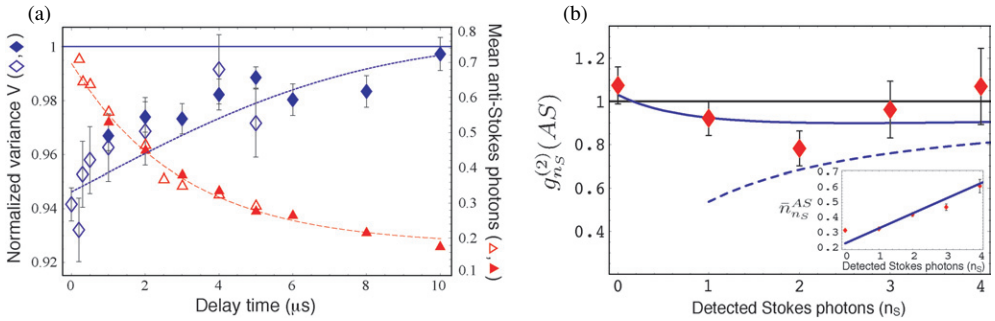

Figure 7. (a) Observation of non-classical correlations. Normalized variance V (diamonds) and mean number of anti-Stokes photons (triangles) versus delay time τ_d. The open and full symbols represent two experimental runs with similar experimental parameters. The dotted line is an exponential fit (characteristic time ~ 3 μs) to the mean number of anti-Stokes photons. The solid line is the result of a theoretical model including the effects of loss, background and several spatial modes on the Stokes and anti-Stokes channels. (b) Conditional non-classical state generation. Diamonds show experimentally measured values $g^{(2)}(AS) = \langle AS_1 \cdot AS_2\rangle / \langle AS_1\rangle\langle AS_2\rangle$ (see figure 5(c)) as a function of the number of detected Stokes photons. The solid line shows the result of a theoretical model including background and loss on both the Stokes and anti-Stokes channels. (Inset) Measured mean anti-Stokes number $\bar{n}^{AS}_{n_S}$ conditioned on the Stokes photon number n_S.

n photons has $g^{(2)} = 1 - 1/n$.) Note that the mean number of anti-Stokes photons grows linearly with n_S, while $g^{(2)}_{n_S}(AS)$ drops below unity, indicating the non-classical character of the anti-Stokes photon states. In the presence of background counts, $g^{(2)}_{n_S}(AS)$ does not increase monotonically with n_S, but exhibits a minimum at $n_S = 2$. The Mandel Q parameter [54] can be calculated using $Q^{AS}_{n_S} = \bar{n}^{AS}_{n_S}\left(g^{(2)}_{n_S}(AS) - 1\right)$; from the measurements we determine $Q^{AS}_{n_S=2} = -0.09 \pm 0.03$ for conditionally generated states with $n_S = 2$ ($Q \geqslant 0$ for classical states and $Q = -1$ for Fock states).

It is evident that the Fock state preparation in these early measurements was far from perfect. We have recently implemented novel technical approaches that allow us to improve mode matching and to combine large signal-to-noise ratio with substantial retrieval efficiencies. Fulfilling these conditions simultaneously is essential for the realization of an efficient, controllable single-photon source as well as for applications in quantum communication. Figure 8(a) shows a novel experimental geometry in which ideal mode matching between the Stokes and anti-Stokes fields can be achieved automatically using single-mode optical fibres. Here, in the ideal limit of plane-wave write and retrieve lasers, the Stokes and anti-Stokes photons are emitted in counter-propagating single modes owing to the phase conjugation property of the underlying four-wave mixing interaction. In such a geometry it is possible to reduce the intensity of the write laser Ω_W such that the probability p of emitting a single Stokes photon from the atomic ensemble is much less than unity. The overall Stokes channel detection efficiency is η, thus making $p\eta$ the detection probability. The condition $p \ll 1$ then guarantees that detection of a single Stokes photon corresponds to no more than a single atomic excitation regardless of losses. Finally, by optimizing the atomic density the various sources of background light can be suppressed. For example, by working in the configuration shown in figure 8(a) we were able to increase the signal-to-noise ratio in the retrieval channel by a factor of 50 by operating at room temperature (20 °C) instead of 75 °C.

The conditional measurements of intensity correlations for generated single photon pulses are shown in figure 8(b). We clearly observe a large degree of suppression of intensity fluctuations $g^{(2)}(AS||n_S = 1) < 1$, indicating the non-classical nature of the anti-Stokes

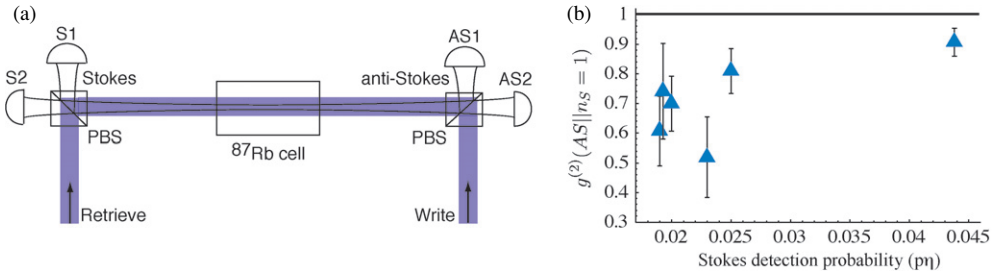

Figure 8. (a) Counter-propagating geometry for mode-matched Stoke/anti-Stokes pair creation. Note that write and retrieve lasers have large beam waist size compared to Stokes/anti-Stokes modes, for ideal phase-conjugate retrieval. (b) Conditional single-photon generation. The second-order correlation function of the anti-Stokes field conditioned on detecting a single Stokes photon, $g^{(2)}(AS||n_S = 1)$, as a function of detection probability $p\eta$ of the anti-Stokes channel. Data taken at an atomic ensemble temperature of 20 °C, black line marks the classical limit $g^{(2)} = 1$.

field, with the lowest observed value $g^{(2)}(AS) = 0.52 \pm 0.14$ occurring with a conditional probability of detecting a single anti-Stokes photon in the relevant mode (retrieval efficiency) of the order of 30%. Since a larger value of p results in a decreased fidelity of preparation, $g^{(2)}(AS||n_s = 1)$ approaches the classical limit of 1 as p increases (see figure 8(b)). Further improvements involving operation at lower excitation power, for example, are likely. These results indicate that the present experimental approach represents a promising avenue for controlled single-photon generation as well as for long-distance quantum communication.

4. Resonantly enhanced nonlinear optics using EIT

4.1. Nonlinear optics at low light level

In general, nonlinear interactions between few-photon pulses are difficult to achieve, as they require a combination of large nonlinearity, low photon loss and tight confinement of the light beams, as well as long atom–photon interaction times [39]. We have suggested recently [40] that the method of stationary light pulses can be extended to confine stationary pulses in all three spatial dimensions (see figure 9(b)), leading to strongly enhanced nonlinear interactions between weak pulses of light using EIT [10]. Specifically an efficient Kerr-like interaction between two pulses can be implemented by exploiting the steep atomic dispersion associated with narrow EIT resonances. In such a system, a small ac Stark shift associated with a weak off-resonant pulse of signal light produces a large change in refractive index for a resonant probe pulse [13]. Coherent, controlled nonlinear processes at optical energies corresponding to a single light quanta appear feasible with this method, as was demonstrated recently [14, 15].

In order to fully exploit these enhanced nonlinear processes, long interaction times between signal and probe pulses must be ensured. Although the latter can be achieved by reducing the group velocities of two interacting pulses by equal amounts [55], in practice this results only in a modest increase of the nonlinear optical efficiency since reduction of the group velocity is accompanied by a corresponding decrease of the light energy in the propagating pulse. Moreover, such a nonlinear interaction is accompanied by pulse distortion, which poses a fundamental limit to the controllability and uniformity of the effective photon–photon interaction. In contrast, the technique presented here allows for long interaction times (associated with stationary light pulses) without proportional reduction of the photon energy and competing effects such as pulse distortion.

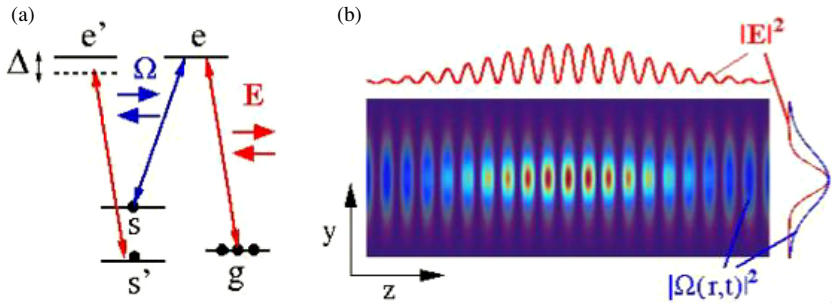

Figure 9. (a) Three-level atoms in Λ-configuration, with auxiliary levels $|s'\rangle, |e'\rangle$. Forward and backward propagating control fields with Rabi frequencies $\Omega_{\pm}$, and weak signal field $\mathcal{E}_{\pm}$. (b) Three-dimensional confinement and waveguiding of signal light due to transverse intensity profile and longitudinal modulation of control field.

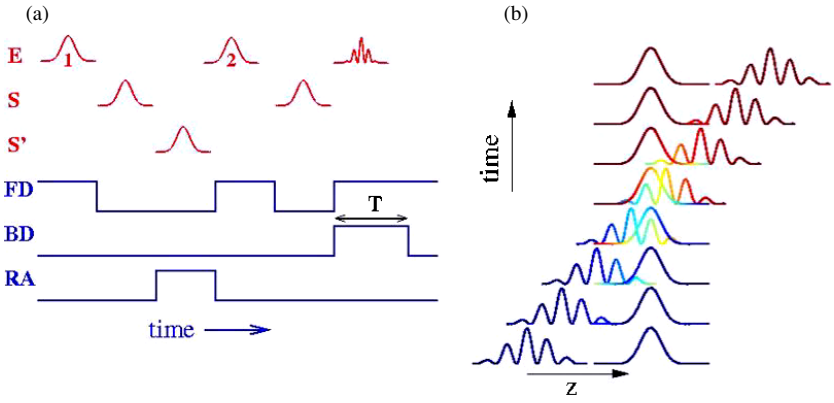

Figure 10. (a) Timing diagram: forward (FD), backward (BD), and Raman or microwave (RA) intensities versus time. The signal pulse (E, 1) is first stored as the spin wave $\mathcal{S}$ and then transferred to $\mathcal{S}'$. Next, the probe pulse (E, 2) is stored as the spin wave $\mathcal{S}$, and then converted to a stationary pulse excitation (E, modulated wavepacket). The stationary and the stored excitation then interact with one another for a time T. (b) Illustration of Kerr interaction between slowly moving stationary probe pulse $\mathcal{S}$ and stored signal pulse $\mathcal{S}'$ leading to a phase shift (represented as changing colour) of pulses.

An effective nonlinear interaction can be achieved as shown in the timing diagram figure10(a). A light signal pulse is initially stored in the $|g\rangle\langle s|$ coherence (see figure 9(a)) for the relevant atomic level configuration). Next, a Raman pulse (RA) or microwave pulse transfers the population from $|s\rangle$ to $|s'\rangle$ (see figure 10(a)), thereby transferring the stored excitation to the coherence $|g\rangle\langle s'|$ (spin wave $\mathcal{S}'$). A second light pulse (probe pulse) is then stored in the $|g\rangle\langle s|$ coherence (spin wave $\mathcal{S}$). The spin excitation associated with the probe pulse is then converted into a stationary excitation, and using unequal intensities in the FD and BD beams, a non-zero group velocity is used to move the stationary probe pulse through the stored spin excitation associated with the signal pulse. Probe light in the modes $\hat{\mathcal{E}}_{\pm}$ interacts dispersively with atoms in level $|s'\rangle$ (see figure 9(a)), thereby acquiring a phase shift proportional to the number of excitations stored in the $|g\rangle\langle s'|$ coherence, leading to an effective Kerr-type nonlinearity. Detailed calculations [40] show that the phase shift is given by $\phi \simeq d_0 \frac{\gamma}{\Delta} \frac{\sigma}{\pi R^2}$, where d_0 is the optical depth, γ is the excited state decay rate, Δ is the

detuning, σ is the resonant absorption cross-section $\sigma = \frac{3}{4\pi}\lambda^2$, and R is the radius of the guided signal mode.

Specifically, for a 100 μm long cloud of cold ^{87}Rb atoms at a density of $n = 10^{13}\,\mathrm{cm}^{-3}$, with an optical depth of $d_0 \simeq 10^3$ and assuming a background index $n_s - 1 \simeq 3 \times 10^{-3}$, we find that by choosing $\gamma/\Delta = 0.1$ (γ is the excited state radiative decay rate and Δ is the detuning of the probe field from $e' - s'$ resonance), a phase shift $\phi_S \sim \pi$ is achievable for a single stored excitation in $|s'\rangle$, while the loss is negligible, at the level of a few per cent.

5. Conclusion and outlook

In summary, we have described several recent advances for generation, storage and manipulation of quantum light pulses using atomic ensembles and electromagnetically induced transparency. These techniques involve manipulating resonant optical properties of an atomic medium, and allow one to coherently control propagation as well as quantum states of weak pulses of light. Although these developments are based on fundamental ideas of quantum theory of light that were formulated by Einstein one hundred years ago and developed in the quantum optics community over the past few decades, the actual developments that we have described here are very recent. While the past few years have seen an exploding interest in this subject, it is clear that many more exciting experiments involving single-photon generation, storage, nonlinear interactions and their applications in quantum communication are still to come.

Acknowledgments

We thank Michal Bajcsy, Lilian Childress, Gene-Wei Li, Jim MacArthur, Florent Massou and Anders Sørensen for their contributions to this work. We gratefully acknowledge discussions with I Cirac, M Fleischhauer, S Harris, A Imamoğlu, M Scully and P Zoller. This work was supported by DARPA, NSF, the Harvard-MIT Center for Ultracold Atoms, the Alfred P Sloan Foundation and the David and Lucille Packard Foundation.

References

[1] Scully M O and Zubairy S M *Quantum Optics* (Cambridge: Cambridge University Press)
[2] Harris S E 1997 *Phys. Today* **50** 36
[3] Field J E, Hahn K H and Harris S E 1991 *Phys. Rev. Lett.* **67** 3062
[4] Hau L V, Harris S E, Dutton Z and Bejroozi C H 1999 *Nature* **397** 594
[5] Budker D, Kimball D F, Rochester S M and Yashchuk V V 1999 *Phys. Rev. Lett.* **83** 1767
[6] Kash M M *et al* 1999 *Phys. Rev. Lett.* **82** 5229
[7] Boyd R W and Gauthier D J 2002 *Progress in Optics* vol 43 (Amsterdam: Elsevier) p 497–530
[8] Lukin M D 2003 *Rev. Mod. Phys.* **75** 457
[9] Marangos J P, Fleischhauer M and Imamoğlu A 2005 *Rev. Mod. Phys.* at press
[10] Lukin M D, Hemmer P R and Scully M O 2000 *Adv. At. Mol. Opt. Phys.* **42** 347
[11] Shverdin M Y, Walker D R, Yavuz D D, Yin G Y and Harris S E 2005 *Phys. Rev. Lett.* **94** 033904
[12] Harris S E, Field J E and Imamoglu A 1990 *Phys. Rev. Lett.* **64** 1107
[13] Harris S E and Hau L V 1999 *Phys. Rev. Lett.* **82** 4611
[14] Zibrov A S, Lukin M D and Scully M O 1999 *Phys. Rev. Lett.* **83** 4049
[15] Braje D A *et al* 2002 *Phys. Rev.* A **68** 041801(R)
[16] Cirac J I, Zoller P, Mabuchi H and Kimble H J 1997 *Phys. Rev. Lett.* **78** 3221
[17] Briegel H-J, Duer W, Cirac J I and Zoller P 1998 *Phys. Rev. Lett.* **81** 5932
[18] Bouwmeester D, Ekert A and Zeilinger A (ed) 2000 *The Physics of Quantum Information* (New York: Springer)
[19] Duan L M, Lukin M D, Cirac J I and Zoller P 2001 *Nature* **414** 413
[20] Childress L, Taylor J M, Sørensen A S and Lukin M D 2004 *Preprint* quant-ph/0410123

[21] Kimble H J 1998 *Phys. Scr.* **76** 127
[22] Kuhn A, Hennrich M and Rempe G 2002 *Phys. Rev. Lett.* **89** 067901
[23] McKeever J, Boca A, Boozer A D, Buck J R and Kimble H J 2003 *Nature* **425** 268
[24] McKeever J *et al* 2004 *Science* **303** 1992
[25] Kozhekin A E, Mølmer K and Polzik E S 2000 *Phys. Rev.* A **62** 033809
[26] Kuzmich A and Polzik E S 2003 *Quantum Information with Continuous Variables* ed S L Braunstein and A K Pati (Dordrecht: Kluwer)
[27] Hammerer K, Mølmer K, Polzik E S and Cirac J I 2004 *Phys. Rev.* A **70** 044304
[28] Fiurášek J, Cerf N J and Polzik E S 2004 *Phys. Rev. Lett.* **93** 180501
[29] Julsgaard B, Sherson J, Cirac J I, Fiurášěk J and Polzik E S 2004 *Nature* **432** 482
[30] Fleischhauer M and Lukin M D 2000 *Phys. Rev. Lett.* **84** 5094
[31] Fleischhauer M and Lukin M D 2002 *Phys. Rev.* A **65** 022314
[32] Liu C, Dutton Z, Behroozi C H and Hau L V 2001 *Nature* **409** 490
[33] Phillips D F *et al* 2001 *Phys. Rev. Lett.* **86** 783
[34] Mair A *et al* 2002 *Phys. Rev.* A **65** 031802(R)
[35] Novikova I *et al* 2004 *Phys. Rev.* A **69** 061802(R)
[36] Akamatsu D, Akiba K and Kozuma M 2004 *Phys. Rev. Lett.* **92** 203602
[37] Bajcsy M, Zibrov A S and Lukin M D 2003 *Nature* **426** 638
[38] Harris S E 1993 *Phys. Rev. Lett.* **70** 552
[39] Boyd R W 2003 *Nonlinear Optics* (San Diego: Academic)
[40] André A, Bajcsy M, Zibrov A S and Lukin M D 2005 *Phys. Rev. Lett.* **94** 063902
[41] Kuzmich A *et al* 2003 *Nature* **423** 731
[42] van der Wal C H *et al* 2003 *Science* **301** 196
[43] Eisaman M D *et al* 2004 *Phys. Rev. Lett.* **93** 233602
[44] Eisaman M D, Massou F, Li G-W, André A, Zibrov A S and Lukin M D in preparation
[45] Chou C W *et al* 2004 *Phys. Rev. Lett.* **92** 213601
[46] Polyakov S V, Chou C W, Felinto D and Kimble H J 2004 *Phys. Rev. Lett.* **93** 263601
[47] Matsukevich D N and Kuzmich A 2004 *Science* **306** 663
[48] Braje D A *et al* 2004 *Phys. Rev. Lett.* **93** 183601
[49] Balic V, Braje D A, Kolchin P, Yin G Y and Harris S E in preparation
[50] Raymer M G and Walmsley I A 1996 *Progress in Optics* vol 28 (Amsterdam: Elsevier) p 181–270
[51] Harris S E, Hoshman M K and Byer R L 1967 *Phys. Rev. Lett.* **18** 732
[52] Hong C K, Ou Z Y and Mandel P 1987 *Phys. Rev. Lett.* **59** 2044
[53] Lukin M D *et al* 1999 *Phys. Rev. Lett.* **82** 1847
[54] Mandel L and Wolf E 1995 *Optical Coherence and Quantum Optics* (Cambridge: Cambridge University Press)
[55] Lukin M D and Imamoğlu A 2000 *Phys. Rev. Lett.* **84** 1419